Cluster Kinetics of Granular Mixing

Benjamin J. McCoy

Dept. of Chemical Engineering, Louisiana State University, Baton Rouge, LA 70803

Giridhar Madras

Dept. of Chemical Engineering, Indian Institute of Science, Bangalore 560 012, India

Granular mixing of identical particles that cluster together is a challenging and important engineering problem. Mixing requires the breakup of clusters, both by individual particle detachment and cluster fragmentation. We apply a population balance (distribution kinetics) approach to describe such size-distributed cluster processes. Expressions for mixing effectiveness and segregation measures are derived and expressed in terms of the rate coefficients for reversible cluster distribution kinetics. Analytical and numerical moment solutions illustrate how the novel method is implemented and also provide some realistic results. The method allows straightforward derivation of experimentally observed long-time power law or exponential asymptotic behavior of segregation metrics for various rate coefficient expressions. © 2005 American Institute of Chemical Engineers *AIChE J,* 51: 406–414, 2005*
*Keywords: granular mixing, cluster distribution, population balance, fluid flow, fragmentation, aggregation*

Introduction

Granular mixing (of powders, sand, seeds, grains, gravel, slurries) is often accomplished by tumbling operations,[1-4] whereby loose particles slide down the inclined surface and/or particle clusters fragment and cascade down the incline (Figure 1). In granular mixing equipment, there are many variations on this theme of splitting and recombining, all with the objective of causing particles to move relative to one another and thus to mix. When interparticle attraction causes clustering, breaking up the clusters is essential to good mixing. When clustering does not occur because cohesion among particles is negligibly small, granular flows are restricted to thin regions.[5] Complications arise when the particles are not uniform because subtle differences in physical properties can cause segregation, such as whether particles differ in density and size.[1] Here we consider identical particles, with some marked as tracers so that mixing can be assessed. Our premise is that the interactions of individual particles and particle clusters that constitute granular mixing can be described quantitatively by addressing the kinetics and dynamics of size-distributed clusters.

The paradigm of continuum mechanics, or mean field theory, cannot easily describe the dynamics of structures and heterogeneities that underlie and strongly influence many processes,[6] including granular mixing, phase transitions, glass dynamics, polymer reactions, turbulence, and other complex systems. Generally, the structures and heterogeneities are dynamic: particles, molecules, or clusters can merge or break apart. We postulate that for many such systems the underlying structural kinetics can be represented quantitatively by population balance (distribution kinetics) modeling. The fundamental processes are breakage and aggregation for clusters and for the irreducible units (particles or monomers) of which they are composed. The monomers are the repeat units in polymerization or depolymerization, the molecules or ions in crystallization, and the particles in granular processes. Population dynamics govern the evolution in time and space for monomer concentration and cluster size distributions. The dynamics of clustering is a fundamental characteristic of granular systems.[7] The purpose of the current investigation is to ascertain how

Correspondence concerning this article should be addressed to B. J. McCoy at bjmccoy@lsu.edu.
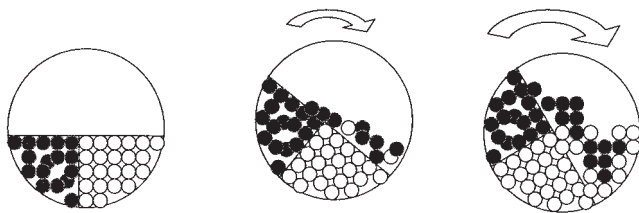
Figure 1. Tumbler mixer with marked tracer particles.

(a) The initial distribution is a cluster of tracer particles separated from the unmarked particles; (b) the tumbler is tilted so that individual loose particles slide down the incline; (c) a larger tilt causes agglomerated clusters to break away and fall down the incline.

well distribution kinetics modeling describes granular system dynamics, in particular, granular mixing.

The physics of granular materials involves a range of conditions,[7] but here we focus on particulates settled in a gravitational field and aggregated by interparticle forces (Figure 1). If the aggregate is tilted slightly, as in a tumbling operation,[4] the individual particles on the surface may detach and slide, as in a surface flow.[2,5] If severely tilted, the aggregate itself may break apart with fragments cascading down as clusters or in a chaotic avalanche.[3,8] These are the processes that allow mixing of powders and particulates. Analysis, design, and control of granular mixing have been difficult because of a lack of understanding of aggregation and breakup for these fundamental processes.[9] Complicating the behavior even more, experimental observations of density relaxation in vibrated granular material suggest clusters having different packing configurations and densities evolve with time.[10] Such identifiable and transforming clusters may behave in a way similar to polymers that transform from one form to another.[11] Population balance modeling successfully handles the polymer case, as well as transformations among crystal polymorphs,[12] and may allow treatment of such evolving granular clusters. Further, unlike computational fluid dynamics or other computer simulations of granular mixing, the distribution kinetics approach is computationally straightforward and rapid, uses fewer parameters, and provides analytical solutions in some cases. Here we treat identical particles under conditions that cause irreversible mixing (decreased segregation). In future work we will extend the concepts to systems of particles differing in size or density that can demix.

The mathematical analysis of complex dynamic processes, such as granular mixing, poses the question of how much detail is needed to describe such systems satisfactorily. Although the answer depends largely on the objectives of the analysis, for most engineering purposes the positions and velocities of each particle as a function of time are not necessary. Similarly, in hydrodynamics, the positions and energy states of each molecule may not be useful if average quantities such as density, fluid velocity, and temperature can be determined. Such average quantities, or moments, are derived, for example, from the Boltzmann equation governing the molecular velocity distribution in gases. In the current approach we have likewise applied a governing (population balance) equation for the cluster size distribution to deduce average properties of the clusters in a granular medium. This has been the general philosophic outlook guiding our approach to complex systems.

The following report begins with a discussion of the kinetics of granular systems applied to mixing. Population balance equations are proposed for the hypothesized cluster breakage–aggregation and particle attachment–detachment processes. A general breakage kernel allowing fragmentation into multiple daughter clusters is postulated. Measures of effectiveness (degree of mixing and scale and intensity of segregation) for mixing of a lump of tracer particles into the granular bulk are defined in terms of moments of the cluster size distributions. Low-order moment solutions allow the consequences of the theory to be evaluated. Relationships to experimental data and other models reveal some underlying features of granular mixing kinetics and dynamics.

Distribution Kinetics

Consider the mixing of identical particles, differentiated only in that the particles to be mixed are marked as tracers (Figure 1). The particles may be detached and free to act as monomers or may reside in clusters held together by gravity and interparticle forces. As in many other systems with structural dynamics,[13,14] granular systems undergo breakage–aggregation or attachment-detachment processes. If $\mathbf{C}(x)$ represents a cluster of mass x and $\mathbf{M}(x_m)$ is a particle (monomer) of mass x_m, we have for reversible monomer dissociation

$$\mathbf{C}(x) \underset{k_g(x)}{\overset{k_d(x)}{\rightleftharpoons}} \mathbf{C}(x - x_m) + \mathbf{M}(x_m) \qquad (1)$$
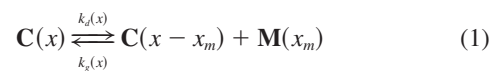
with rate coefficients k_g and k_d for cluster growth (attachment) and dissociation (detachment), respectively. The clusters may also fragment with breakage rate coefficient k_b, or aggregate with rate coefficient k_a

$$\mathbf{C}(x) \underset{k_a}{\overset{k_b(x)}{\rightleftharpoons}} \mathbf{C}(x') + \mathbf{C}(x - x') \qquad (2)$$
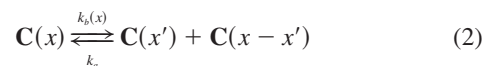
In granular systems the rate coefficients are related to the constituency of the particles. If the system is dry and the particles flow freely, then $k_d > k_g$ and $k_b > k_a$, whereas if the particles clump together (typically because they are wet), the reverse inequalities may hold. The rate coefficients are also functions of imposed motion (agitation), which takes the place of temperature[14,15] in molecular systems. Agitation may occur by vessel motion through shaking or repeated vessel inversion, or by imposed forces within the vessel through motion of an impeller or flow of fluid through the particulates (fluidized bed). Imperfect mixing may be the result of restricted agitation, as in overfilling.[1] We consider that k_b and k_d decrease with cohesion among particles and increase with agitation. In the absence of agitation, if $k_d \ll k_g$ and $k_b \ll k_a$, then a single intact cluster, possibly with fault lines and defect surfaces, settles to a stationary lump. If agitation is extremely energetic then the reverse inequalities will hold, $k_d \gg k_g$ and $k_b \gg k_a$, and all the particles will move freely because all clusters will be disintegrated. Solving the population balance equations for the cluster size distribution and the monomer concentration, $c(x, t)$ and $m^{(0)}(t)$, respectively, yields their time-dependent behavior. The time evolution is important in mixing, where an initial cluster distribution of tracer particles is to be dispersed throughout the other particles.

By analogy with fluids, granular mixing has been character-

ized as combining convection and diffusion.[1] If the diffusion occurs at cluster interfaces, similar to fluid mixing,[16] this approach would yield a Damkohler number incorporating diffusivity. Defining such a diffusion coefficient for a hydrodynamic model of compacted particulate systems may be questioned.[6] An alternative approach is the particulate theory suggested above with Eqs. 1 and 2. The key feature is to recognize the granular nature of the particulate system, for which the fundamental processes are cluster breakage–aggregation and growth–dissociation processes. Thus, fluid mechanics equations based on mean-field continuum models might not accurately describe granular systems, which inherently possess structural heterogeneities.[6] The advantage of population balance, or distribution kinetics modeling, is that Eqs. 1 and 2 mathematically describe dynamic heterogeneities and structural features. Separate regions of cluster and particulate motion characterize the flow of granular materials. Generally, the regions are dynamic, with individual particles moving between the cluster and particle regimes according to Eq. 1. We consider that the clusters are sufficiently rigid that particles can detach from a cluster only at its surface, and not by burrowing out from below the surface. The clusters transform by fracturing, thus breaking into smaller clusters with particles detaching from the new surfaces formed at the fracture interface. The free particles allow relative movement of the fragmented clusters.

This view is consistent with sand pile dynamics.[7] For stationary piles, particulate flow is restricted to thin layers on the surface of the pile,[5] as suggested in Figure 1b. If the particles are agglomerated and the pile is tipped to a steeper angle, or perturbed possibly by small jolts accompanying the thin film flows, clusters may fracture from the pile and cause avalanches of combined cluster and particle movement (Figure 1c).

Equation 1 explains how sand pours as individual particles through the narrow opening of an hourglass.[15] Gravitational force causes separate particles to break from the arched cluster surface nearest the passageway. As the arched cluster is eroded away, clusters fracture and fall to take its place. The presence of chainlike clusters[7] and consequent arching, or vaulting, explains why pressure does not depend on the depth of particles. Particle flow rate through the opening is therefore not affected by the height of sand, allowing the hourglass to empty itself in a reproducible time.

Population balance modeling

Consider identical particles of mass x_m, some marked as tracers, that may be aggregated into clusters (Figure 1). A future study will address particles differing in size or density. The population balance equations that govern the distribution of the clusters, $c(x, t)$, and of the particles, $m(x, t) = m^{(0)}(t)\delta(x - x_m)$, are based on mass conservation[13] for the processes represented by Eqs. 1 and 2

$$\partial c(x, t)/\partial t = -k_g(x)c(x, t)\int_0^\infty m(x', t)dx'$$

$$+ \int_0^x k_g(x - x')c(x - x', t)m(x', t)dx'$$

$$- k_d(x)c(x, t) + \int_x^\infty k_d(x')c(x', t)\delta[x - (x' - x_m)]dx'$$

$$- 2k_a c(x, t)\int_0^\infty c(x', t)dx' + k_a\int_0^x c(x', t)c(x - x', t)dx'$$

$$- k_b(x)c(x, t) + \int_x^\infty k_b(x')c(x', t)\Omega(x, x')dx' \quad (3)$$

and

$$\partial m(x, t)/\partial t = -m(x, t)\int_0^\infty k_g(x')c(x', t)dx'$$

$$+ \int_x^\infty k_d(x')c(x', t)\delta(x - x_m)dx' \quad (4)$$

Dirac delta distributions of fragmentation products, $\delta[x - (x' - x_m)]$ and $\delta(x - x_m)$, represent the monomer removal kernels[17] in Eqs. 3 and 4. We have assumed k_a is constant and the other three rate coefficients are functions of x.

Fragmentation kernels

Breakage into multiple unequal sized clusters is represented by

$$C(x) \xrightarrow{k_b} C(x') + C(x'') + \cdots + C(x - x' - x'' - \cdots)$$

which replaces the forward process in Eq. 2. According to Diemer and Olson,[18] the following breakage kernels with $q \geq 0$ can be formulated for breakage into unequal fragments:

Power-Law Product

$$\Omega(x, x') = N\Gamma(Nq)/[\Gamma(q)/\Gamma(qN - q)]$$
$$\times (x/x')^{q-1} \times (1 - x/x')^{q(N-1)-1}/x \quad (5a)$$

Power-Law Sum

$$\Omega(x, x') = N[N^{-1}(x/x')^{q-1}(1 - x/x')^{N-2}/B(q, N - 1)$$
$$+ (1 - 1/N)(1 - x/x')^{q+N-3}/B(1, q + N - 2)]/x' \quad (5b)$$

in terms of the number of daughters, N, and the beta function, $B(a, b) = \Gamma(a)\Gamma(b)/\Gamma(a + b)$. Equations 5a and 5b are extensions of earlier work by Hill and Ng,[19] and reduce to most if not all known fragmentation kernels.[18] The random binary fragmentation kernel is $\Omega(x, x') = 2/x'$, which holds if $N = 2$ and $q = 1$. When q becomes infinite, the kernel for breakage into N equal-sized fragments is $\Omega(x, x') = N\delta(x - x'/N)$. Noncohesive particles, such as dry sand, are expected to have a large value of N.

Integral forms of the rate expressions in the population

balances lend themselves to calculations by moments, defined as integrals over mass x

$$c^{(n)}(t) = \int_0^\infty c(x, t)x^n dx \qquad (6)$$

The zeroth moment, $c^{(0)}(t)$, is the time-dependent number of clusters per total particulate volume, and the first moment, $c^{(1)}(t)$, is mass concentration (mass/volume) of clusters. The average cluster mass is the ratio

$$c^{\text{avg}} = c^{(1)}/c^{(0)} \qquad (7)$$

Although we use only these lower moments for the present treatment of granular mixing, measures of cluster polydispersity based on the second moment can also be defined.[13,14]

Rate coefficients

Surface-controlled attachment or detachment of particles to clusters can be expressed in terms of particle mass x, as follows

$$k_g(x) = \kappa_g x^\lambda \qquad \text{and} \qquad k_d(x) = \kappa_d x^\lambda \qquad (8)$$

The (nonfractal) cluster area is proportional to $x^{2/3}$, so $\lambda = 2/3$ represents attachment limited by particle deposition and dissociation at the cluster surface. If deposition and dissociation are independent of the surface area, then $\lambda = 0$, such as for loose, dry particles or for high-liquid-content slurries.[20] Because cohesive particles will dissociate or deposit only at cluster surfaces, $\lambda \leq 2/3$ is the expected value. The breakage rate coefficient may also increase with increased particle mass, $k_b(x) = \kappa_b x^\nu$. For cohesive particles $\nu > 0$ is expected, so that cluster fragmentation increases with cluster size; however, for free-flowing particles, such as dry sand, $\nu = 0$ is more likely. Recognizing that fragmentation rather than aggregation is the focus of mixing, we allow k_a to be approximated as constant with x.

With mass-dependent rate coefficients the population balance equation for the cluster size distribution is[13]

$$\partial c(x, t)/\partial t = -\kappa_g x^\lambda c(x, t)m^{(0)}(t) + \kappa_g(x - x_m)^\lambda$$
$$\times \ c(x - x_m, t)m^{(0)}(t) - \kappa_d x^\lambda c(x, t) + \kappa_d(x + x_m)^\lambda c(x + x_m, t)$$
$$- 2k_a c(x, t)c^{(0)}(t) + k_a \int_0^x c(x', t)c(x - x', t)dx' - \kappa_b x^\nu c(x, t)$$
$$+ \kappa_b \int_x^\infty x'^\nu c(x', t)\Omega(x, x')dx' \qquad (9)$$

If Eq. 5 is used as the kernel for breakage into N equal-sized fragments, then the last term in Eq. 9 is $N\kappa_b(xN)^\nu c(x, t)$.

According to Eq. 4 the concentration (0th moment) of detached particles is governed by

$$dm^{(0)}/dt = [\kappa_d - \kappa_g m^{(0)}]c^{(\lambda)} \qquad (10)$$

and mass conservation requires that $dc^{(1)}/dt + x_m dm^{(0)}/dt = 0$. The moment equation[11] for Eq. 9 is

$$dc^{(n)}/d\theta = -\kappa_g m^{(0)}c^{(n+\lambda)} + \kappa_g m^{(0)}\sum_{j=0}^n \binom{n}{j}c^{(n-j+\lambda)}(x_m)^j$$
$$- \kappa_d c^{(n+\lambda)} + \kappa_d \sum_{j=0}^n \binom{n}{j}c^{(n-j+\lambda)}(-x_m)^j - 2k_a c^{(0)}c^{(n)}$$
$$+ k_a \sum_{j=0}^n \binom{n}{j}c^{(n-j)}c^{(j)} + \kappa_b c^{(n+\nu)}[g(n, q) - 1] \qquad (11)$$

where

$$g(n, q) = N\Gamma(n + q)\Gamma(qN)/[\Gamma(q)\Gamma(n + Nq)] \qquad (12)$$

which by the properties of a breakage kernel is constrained for $n = 0$ and 1 to equate to the number of daughters N and to 1, respectively,[18]

$$g(0, q) = N \qquad \text{and} \qquad g(1, q) = 1 \qquad (12a)$$

This ensures that the mass balance is satisfied, so that $c^{(1)}(t) + x_m m^{(0)}(t)$ is constant independently of the values of ν and λ.

Mixing

A mixing process is illustrated by dispersal of a lump of tracer particles into a vessel of unmarked but otherwise identical particles. Other initial conditions are of course possible, but here we consider a single cluster of tracer particles that will be mixed into the bulk particles by breakage and particle detachment at the cluster interface, as occurs in a tumbling process. The initial tracer cluster with mass c_0^{avg} has the distribution given by

$$c(t = 0, x) = c_0(x) = c_0^{(0)}\delta(x - c_0^{\text{avg}}) \qquad (13)$$

The initial mass per total volume occupied by *all* particles is $c_0^{(1)} = c_0^{(0)}c_0^{\text{avg}}$ and if ρ is the density of single particles, then $c_0^{(1)}/\rho$ is the volume fraction of tracer particles. The number of tracer particles per total volume for the initial cluster is $c_0^{(1)}/x_m$, which is conserved in batch mixing. The mass balance on the tracer particles relates the initial to the time-dependent cluster density and separate particle concentration, and also to the final state

$$c_0^{(1)} = c^{(1)}(t) + x_m m^{(0)}(t) \approx x_m m_f^{(0)} \qquad (14)$$

The subscript f refers to the final mixed state where the tracer particles are dispersed within the bulk, implying that the initial cluster has been totally fragmented into individual particles and $c_f^{(1)} \approx 0$. Thus, the initial cluster is predominantly dispersed into separate particles by granular mixing.

According to this notion, a measure of mixing, the mixing effectiveness, can be defined as the degree of dispersal at any time

$$S(t) = m^{(0)}(t)/m_f^{(0)} \qquad (15)$$

This quantity also measures the intensity of segregation, defined as $1 - S = C^{(1)}$, indicating the dispersal of individual particles.[21] For granular mixing as portrayed here, particle dissociation rather than diffusion is the dispersal mechanism. Initially, before any mixing occurs, $m^{(0)}(t) = 0$ and $S = 0$, and when dispersal is complete, $m^{(0)}(t) = m_f^{(0)}$ and $S = 1$. By the mass balance, Eq. 14, this is equivalent to

$$S(t) = 1 - [c_0^{(1)} - x_m m^{(0)}(t)]/c_0^{(1)} = x_m m^{(0)}(t)/c_0^{(1)}$$
$$= 1 - c^{(1)}(t)/c_0^{(1)} \qquad (16)$$

In addition to the intensity of segregation or mixing effectiveness, another metric is the scale of segregation, which quantifies the degree to which tracer clusters are fragmented by assessing the size of clusters of unmixed tracer.[21] At time t the number of tracer particles in an average cluster is $c^{\mathrm{avg}}(t)/x_m = C^{\mathrm{avg}}(\theta)$, which is dimensionless and thus quantifies the scale of segregation. During granular mixing, $C^{\mathrm{avg}}(\theta)$ will decline from its large initial value to nearly unity when tracer clusters are totally fragmented into individual tracer particles after a long time. A normalized scale of segregation may be defined as $C^{\mathrm{avg}}(\theta)/C_0^{\mathrm{avg}}$, which decreases from 1 to nearly 0.

Estimating mixing effectiveness at any time thus involves computation of the three moments, $m^{(0)}(t)$, $c^{(0)}(t)$, and $c^{(1)}(t)$, or equivalently, $S(\theta)$ and $C^{\mathrm{avg}}(\theta)/C_0^{\mathrm{avg}}$. The intensity and scale of segregation are measures of particle dispersal and cluster breakup, respectively, as represented by Eqs. 1 and 2. Estimating such mixing effectiveness and segregation metrics from experimental data, however, is nontrivial[22] because of spatial inhomogeneities. The present model is based on an assumption that the clusters and particles are well mixed, which has the advantage of simplifying the mathematics, but may not be as realistic as computer simulations that track the spatial evolution of the heterogeneities.

Moment equations

The first few moments can be obtained from Eq. 11. For $n = 0$, 1, and 2, with Eq. 12a, Eq. 11 becomes

$$dc^{(0)}/dt = \kappa_b(N-1)c^{(\nu)} - k_a c^{(0)2} \qquad (17)$$

$$dc^{(1)}/dt = x_m c^{(\lambda)}[-\kappa_d + \kappa_g m^{(0)}] \qquad (18)$$

$$dc^{(2)}/dt = x_m^2 c^{(\lambda)}[\kappa_g m^{(0)} + \kappa_d] + 2x_m c^{(1+\lambda)}[-\kappa_d + \kappa_g m^{(0)}]$$
$$+ 2k_a c^{(1)2} + \kappa_b c^{(2+\nu)}[g(2,q) - 1] \qquad (19)$$

The properties of the kernel (Eq. 12a) require that the zeroth and first moments are independent of the shape of the daughter distribution. It follows that Eqs. 10 and 18 satisfy the mass balance, $x_m dm^{(0)}/dt = -dc^{(1)}/dt$, consistent with Eq. 14. The mixing efficiency is determined by substitution (Eq. 16) and requires only lower moments $n = 0$ and 1. When ν is nonzero, no analytical solutions exist for Eqs. 17 and 18. For $\nu = 0$, analytical solutions are possible and the final state for this reversible system is an equilibrium condition determined by setting the time derivatives in Eqs. 10 and 17 to zero

$$m_f^{(0)} = \kappa_d/\kappa_g \qquad \text{and} \qquad c_f^{(0)} = (N-1)\kappa_b/k_a \qquad (20)$$

According to Eq. 14, good mixing requires that clusters are broken up, that is, $x_m m_f^{(0)} \gg c_f^{(1)}$, such that for small final clusters we have $c_f^{(1)} \approx x_m c_f^{(0)}$, and therefore $m_f^{(0)} \gg x_m c_f^{(0)}$. The case $\nu = 1$, which requires a numerical solution for the $n = 0$ and 1 moments, has the equilibrium conditions

$$m_f^{(0)} = \kappa_d/\kappa_g \qquad \text{and} \qquad c_f^{(0)} = [(N-1)c_f^{(1)}\kappa_b/k_a]^{1/2} \qquad (21)$$

Dimensionless equations

To minimize the number of parameters, we define the dimensionless quantities

$$C^{(n)} = c^{(n)}/m_f^{(0)}x_m^n \qquad \theta = t\kappa_d x_m^\lambda \qquad \beta = \kappa_b/\kappa_d x_m^{\lambda+\nu}$$

$$S = m^{(0)}/m_f^{(0)} \qquad \alpha = k_a m_f^{(0)}/\kappa_d x_m^\lambda = k_d/\kappa_g x_m^\lambda \qquad (22)$$

All rates are scaled by the monomer dissociation rate coefficient, $\kappa_d x_m^\lambda$. Relating each rate term as a ratio allows a comparison of competitive rates of cluster fragmentation or breakage (β), and aggregation (α). The differential Eqs. 10, 17, and 18, when divided by $x_m^{n+\lambda}\kappa_d m_f^{(0)}$, yield the following dimensionless differential equations

$$dC^{(0)}/d\theta = (N-1)\beta C^{(\nu)} - \alpha C^{(0)2} \qquad (23)$$

$$dC^{(1)}/d\theta = (S-1)C^{(\lambda)} = -dS/d\theta \qquad (24)$$

According to the present theory, Eqs. 23 and 24 are the governing equations for granular mixing dynamics. The initial conditions are

$$S(\theta = 0) = 0 \qquad C^{(1)}(\theta = 0) = C_0^{(1)} \qquad C^{(0)}(\theta = 0) \approx 0 \qquad (25)$$

the last of which derives from $C_0^{(0)} = c_0^{(0)}/m_f^{(0)} = 1/(\text{total number of particles}) \approx 0$. In the computations described below, $C^{(0)}(\theta = 0) = 0.0001$. The symmetry of Eq. 24 gives $d[S + C^{(1)}]/d\theta = 0$, and thus the mass balance

$$C_0^{(1)} = S(\theta) + C^{(1)}(\theta) = 1 \qquad (26)$$

Based on Eq. 26, Eq. 24 can be rewritten as

$$dC^{(1)}/d\theta = -C^{(1)}C^{(\lambda)} \qquad (27)$$

For $\lambda = 1$, the solution for Eq. 27 is

$$C^{(1)}(\theta) = 1/(1 + \theta) \qquad (28)$$

and the long time asymptote is the power law, $C^{(1)}(\theta) \sim \theta^{-1}$. The mixing efficiency for $\lambda = 1$ is

$$S = \theta/(1 + \theta) \qquad (29)$$

Table 1. Asymptotic Long-Time Behavior of the Scaled Number Concentration $C^{(0)}(\theta)$, the Scaled Number Concentration or Intensity of Segregation $C^{(1)}(\theta)$, and the Scale of Segregation $C^{\mathrm{avg}}(\theta)/C_0^{\mathrm{avg}}$

Variable	$\nu = \lambda = 0$	$\nu = 0, \lambda = 1$	$\nu = \lambda = 1$	$\nu = 1, \lambda = 0$
$\mathbf{C}^{(0)}(\theta)$	$(N - 1)\beta/\alpha$	$(N - 1)\beta/\alpha$	$\theta^{-1/2}$	θ^{-1}
$\mathbf{C}^{(1)}(\theta)$	$\exp[-\theta(N - 1)\beta/\alpha]$	θ^{-1}	θ^{-1}	θ^{-2}
$\mathbf{C}^{\mathrm{avg}}(\theta)/\mathbf{C}_0^{\mathrm{avg}}$	$\exp[-\theta(N - 1)\beta/\alpha]$	θ^{-1}	$\theta^{-1/2}$	θ^{-1}

which is a simple function of $\theta = tk_d$, and thus is independent of N, α, and β.

For $\nu = 0$ and with the initial condition, $C^{(0)}(\theta = 0) = C_0^{(0)}$, the solution of Eq. 23, the logistic equation, is independent of λ

$$C^{(0)}(\theta) = C_0^{(0)}(N - 1)\beta e^{(N-1)\beta\theta}[(N - 1)\beta$$
$$+ C_0^{(0)}\alpha\{e^{(N-1)\beta\theta} - 1\}]^{-1} \quad (30)$$

The scale of segregation is then $C^{\mathrm{avg}}(\theta) = 1/[(1 + \theta)C^{(0)}(\theta)]$. The equilibrium final conditions for $\nu = 0$ (Eq. 21), defined when time derivatives in Eqs. 23 and 24 vanish, are

$$S_f = 1 \quad \text{and} \quad C_f^{(0)} = (N - 1)\beta/\alpha \quad (31)$$

An analytical solution for $\lambda = \nu = 0$ is also feasible, and as mentioned above may be realistic for mixing noncohesive particles. When Eq. 30 is substituted into Eq. 24 for $\lambda = 0$ and solved with the initial condition, $C^{(1)}(\theta = 0) = 1$, one obtains

$$C^{(1)}(\theta) = [C_0^{(0)}(-1 + e^{\beta(N-1)\theta})\alpha/\{(N - 1)\beta\} + 1)]^{-1/\alpha} \quad (32)$$

Thus for $\lambda = \nu = 0$, the solution is given by Eqs. 30 and 32 with parameters N, α, and β. If $N \gg 1$ and the exponential term dominates, then Eq. 32 reduces to

$$C^{(1)}(\theta) \approx (N\beta/\alpha C_0^{(0)})^{1/\alpha}e^{-N\beta\theta/\alpha} \quad (33)$$

This can be compared to expressions derived for liquids,[16] which were also exponential in time. The exponential time dependency is typical of noncohesive granular mixing,[8,22] suggesting that a fluid dynamics model should approximate mixing in free-flowing granular systems. Segregation arising from particle size or density differences, however, can cause $C^{(1)}$ to level off and reach a constant value.

The cases $\nu = 1$ and $\lambda = 0$ or 1 require relatively straightforward numerical solutions of ordinary differential equations. For $\nu = \lambda = 1$, we substitute Eq. 28 for $C^{(1)}$ and solve the nonlinear ordinary differential equation numerically as

$$dC^{(0)}/d\theta = (N - 1)\beta/(1 + \theta) - \alpha C^{(0)2} \quad (34)$$

For $\nu = 1$ and $\lambda = 0$, the two simultaneous equations are solved numerically

$$dC^{(0)}/d\theta = (N - 1)\beta C^{(1)} - \alpha C^{(0)2} \quad (35)$$

$$dC^{(1)}/d\theta = -C^{(1)}C^{(0)} \quad (36)$$

The initial conditions are given by Eq. 25. For an extended time the 0th moment according to Eq. 23 is $C^{(0)} \sim [C^{(1)}(N -$

$1)\beta/\alpha]^{1/2}$, which can be substituted into Eq. 36. Integrating the resulting asymptotic equation yields the power-law dependency on time, $C^{(1)} \sim \theta^{-2}$ for $\theta \gg 1$.

Table 1 summarizes the asymptotic results that were derived analytically and confirmed by the numerical computations. The powers on time depend only on the values ν and λ, independent of the rate coefficient magnitudes. The discrete nature of granular systems implies that clusters may be completely fragmented, which places an upper limit on time θ. As particle size becomes infinitesimally small, however, θ can increase without limit.

Results and Discussion

The present analysis reveals some insights into scaling, a central issue in all mixing processes. Ottino and Khakhar[5] showed how free-flowing particles are restricted to thin regions in granular flows. Clustering complicates the physics, but we have demonstrated that the distribution kinetics approach yields governing equations with dimensionless parameters, a requirement for scaling. For the case $\nu = 0$, Eq. 23 contains the basic information. The final number of tracer clusters is given by the stationary state

$$C_f^{(0)} = (N - 1)\beta/\alpha = (N - 1)(k_b/k_a)(\kappa_g/\kappa_d) \quad (37)$$

in which all rate coefficients appear. The actual number of clusters at any time is

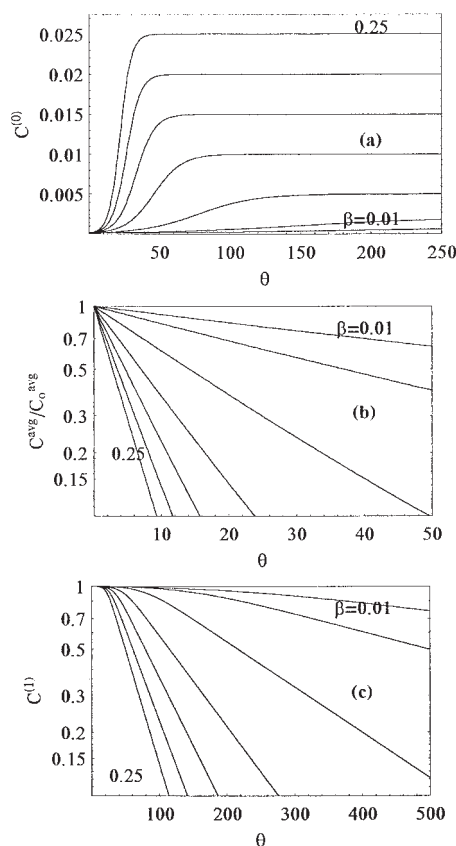$$c^{(0)}(t) = C^{(0)}(\theta)\kappa_d/\kappa_g \quad (38)$$

increasing with the ratio of dissociation to growth rates. The mixing time depends on the particle size, x_m

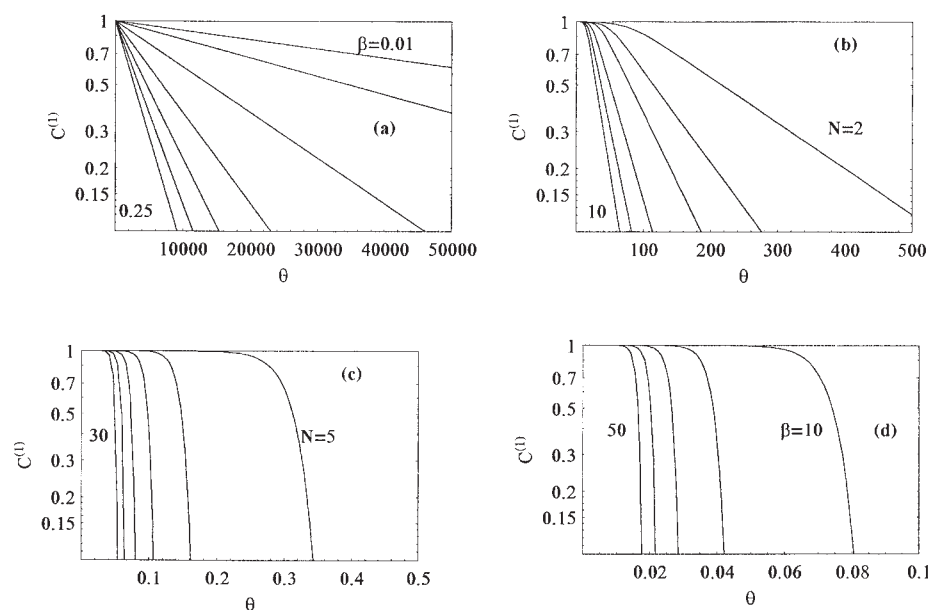$$t = \theta/(\kappa_d x_m^\lambda) \quad (39)$$

increasing as x_m decreases, so that larger particles mix faster. Fine powders, therefore, would generally require a longer time to mix.

The interpretation of the rate coefficients in Eqs. 1 and 2 suggests how values of α, β, and N are related to practical granular systems. When dry particles are mixed they readily dissociate from clusters, which also are easily fragmented ($N \gg 1$); thus α is small and β is quite large. Wet cohesive particles stick together so that α is large and N is a small integer greater than unity. As explained above, $0 \le \lambda \le 1$ and $0 \le \nu \le 1$ define reasonable values, and thus our mixing results bracket this range. We first report results for $\nu = 0$, for which solutions can be obtained analytically in closed form.

For $\nu = \lambda = 0$, Eqs. 30 and 32 are key results displayed graphically in Figure 2. For $N = 2$, the scaled cluster number concentration and normalized scale of segregation with time are plotted in Figures 2a and b for $\alpha = 10$ and various values of β. The variation of the normalized scale of segregation with

Figure 2. For $\nu = \lambda = 0$, the time evolution of (a) scaled cluster number concentration; (b) normalized scale of segregation; (c) intensity of segregation for $\beta = 0.01, 0.02, 0.05, 0.1, 0.15, 0.2,$ and 0.25.

The other parameters are $N = 2$ and $\alpha = 10$.

time is nearly linear on a semilogarithmic plot. The segregation intensity, Eq. 32, depends on α, β, and N, as shown in Figure 2c. For fixed N and α, $C^{(1)}$ decreases faster with increasing β. For fixed α and β, $C^{(1)}$ would decrease faster with increasing N.

Figures 3a–d show the time variation of the intensity of segregation, $C^{(1)}$, for various values of α, β, and N. For fixed N and β, the time dependency of the intensity of segregation for large α ($=1000$) (Figure 3a) is similar to that of smaller α (Figure 2c). Figures 3b–d indicate that the segregation intensity decreases faster with increasing β and N. Figures 3c and d depict the case of dry particles, wherein α is small ($=0.01$), for large values of β and N, respectively. Similar to previous results, $C^{(1)}$ decreases faster with increasing β and N.

For $\nu = 0$ and $\lambda = 1$, the solution for the number concentration is given by Eq. 30 and for mass concentration by Eq. 28. The number concentration $C^{(0)}(\theta)$ is represented in Figure 2a. The normalized scale of segregation $C^{\mathrm{avg}}(\theta)/C_0^{\mathrm{avg}}$ (Figure 4a) for $\alpha = 10$, $N = 2$, and various values of β decrease with time, becoming asymptotically the power dependency, θ^{-1}. The intensity of segregation, $C^{(1)}$, Eq. 28, is independent of α, β, and N (Figure 4b) and also decreases as θ^{-1}. Such power-law behavior has been observed in experiments with dextrose and wet kaolinite.[20,22] Michaels and Puzinauskas[20] found the power on time was between -0.7 and -1.2, in general agreement with our computed results.

We next present results for $\nu = 1$, for which solutions are obtained by numerically solving Eq. 34 for $\lambda = 1$ and Eqs. 35 and 36 for $\lambda = 0$. For $\nu = 1$ and $\lambda = 0$, the number concentration reaches a maximum with power law dependency on either side of the maximum (Figure 5a). The normalized scale of segregation, $C^{\mathrm{avg}}(\theta)/C_0^{\mathrm{avg}}$ (Figure 5b), decreases with time in a way that is influenced by the number concentration maximum, but eventually attains an asymptotic power law. The intensity of segregation (Figure 5c) decreases faster with increasing β with slope -2 on the log–log coordinates. For $\nu = $

Figure 3. For $\nu = \lambda = 0$, the time dependency of the intensity of segregation for (a) $\alpha = 1000$ and $\beta = 0.01, 0.02, 0.05, 0.1, 0.15, 0.2,$ and 0.25 with $N = 2$; (b) $\alpha = 10$, $\beta = 0.05$, and $N = 2, 3, 4, 6, 8,$ and 10; (c) $\alpha = 0.001$, $\beta = 1$, and $N = 5, 10, 15, 20, 25, 30$; (d) $\alpha = 0.01$, $N = 20$ and for $\beta = 10, 20, 30, 40,$ and 50.

$\lambda = 1$, the number concentration reaches a maximum (Figure 6a), similar to that observed in Figure 5a, but the long-time asymptote is influenced more by β. Scale of segregation decreases in two power-law regimes also because of $C^{(0)}(\theta)$. The intensity of segregation for $\lambda = 1$ is independent of ν and is illustrated in Figure 4b. The results indicate that the mixing effectiveness S rises rapidly (the intensity of segregation, $C^{(1)} = 1 - S$, decreases) because particles dissociate from the clusters at a rate that is faster for larger clusters. The mixing effectiveness eventually reaches unity ($C^{(1)}$ becomes vanishingly small) as smaller clusters are dissociated over a longer time period. The exponential time dependence means that most mixing occurs early in the process. The transition to power-law time dependence indicates decreased mixing efficiency.
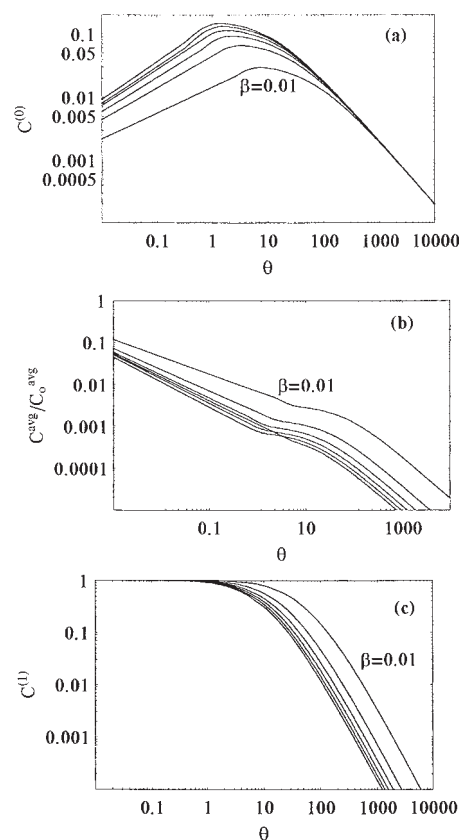
A principal finding of our investigation is that the exponents on cluster mass for the rate coefficients govern the time dependence of segregation. The metrics show exponential time dependence for early time, transitioning to power-law dependence. The exception is the simplest case with $\nu = \lambda = 0$, which is exponential in time and may be realistic for dry powders. The exponential dependence for small values of time has been previously reported. The data of Khakhar et al.[23,24] (see also McCarthy et al.[8]) shift from exponential to power law. Reported computer simulations also show such a transition.[8,23,24] Although the present model describes identical particles, the cited data and simulations are for systems with particle density differences, which prevent complete mixing. Our results show that the time of the transition to power-law dependence depends on the magnitudes of rate coefficients. Decreasing β or N or increasing α increases the time of the transition.

Clearly in this kinetic rate theory, the rate coefficient magnitudes and their cluster-mass dependence are fundamental. Relating the coefficients to particle properties (interparticle forces, wetness, particle shape) is a difficult matter, similar to relating rate constants in chemical reaction kinetics to molec-
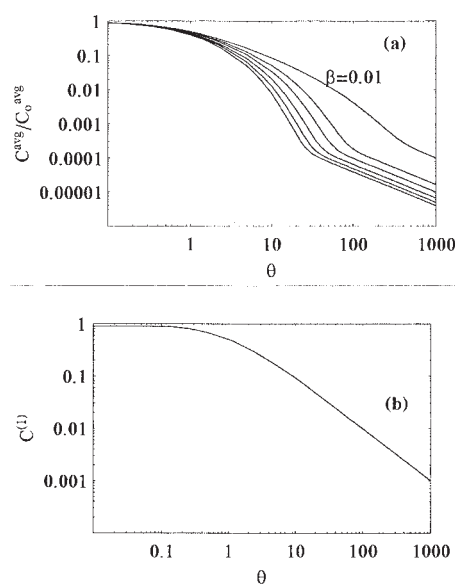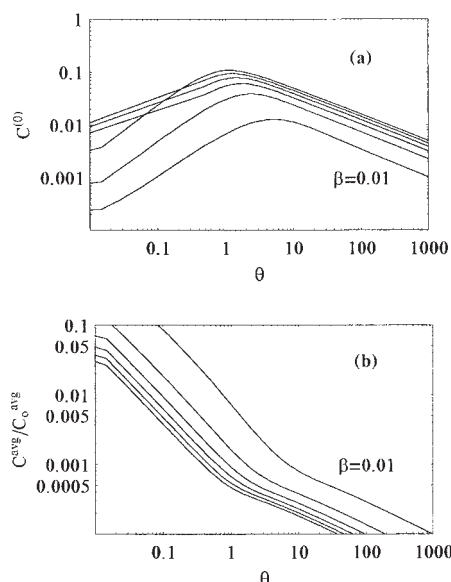

Figure 5. For $\nu = 1$ and $\lambda = 0$, the evolution of (a) scaled cluster number concentration; (b) normalized scale of segregation; (c) intensity of segregation for $\beta = 0.01$, 0.02, 0.05, 0.1, 0.15, 0.2, and 0.25, $N = 2$, and $\alpha = 10$.

ular properties. McCarthy et al.[8] suggest a capillary force approach to characterize particle cohesion. It is also possible that experimentally measuring mixing times in laboratory systems will allow fitting experimental mixing curves to determine coefficients or their ratios. Our results suggest that if asymptotic behavior can be monitored, this would allow discrimination of the rate coefficient mass dependency.

Conclusions

In a new approach to granular materials, we have investigated the application of population balance (distribution kinetics) modeling to granular mixing. The central concept in this treatment is the interaction of cluster-size distributions and single-particle (monomer) concentrations. The aggregation–fragmentation and growth–dissociation of monomer–cluster systems is a common theme in physical and chemical phenomena. Such dynamical systems can be effectively addressed through population balance modeling, as demonstrated here. Among the premises that guided our thinking about granular mixing are the following. All particles are identical, aside from tracer markings, so that size and density differences do not contribute to segregation tendencies. Gravity is always present, forcing the particles to settle and aggregate in the absence of measures to prevent aggregation. In addition to gravitational settling, attractive forces among particles may induce their agglomeration. The method of agitation is con-

Figure 4. For $\nu = 0$ and $\lambda = 1$, the time dependency of (a) normalized scale of segregation for $\beta = 0.01$, 0.05, 0.1, 0.15, 0.2, and 0.25; (b) intensity of segregation (independent of α, β, and N).

The other parameters are $N = 2$ and $\alpha = 10$.

Figure 6. For $\nu = \lambda = 1$, the time evolution of (a) scaled cluster number concentration and (b) normalized scale of segregation for $\beta = 0.01, 0.02, 0.05, 0.1, 0.15, 0.2,$ and 0.25.

The other parameters are $N = 2$ and $\alpha = 10$.

sidered a tumbling operation, allowing free particles to flow in a thin layer and clusters of particles to break away and avalanche down the incline. Multiple fragmentation (daughter) products are incorporated in general expressions for the breakage kernel. Given the observed fragmentation and single-particle flows during tumbling of granular materials, it is plausible that mixing can be described quantitatively by the kinetics of cluster size distributions as implemented by population balance modeling. Interestingly, the particle dissociation and cluster fragmentation processes of Eqs. 1 and 2 correspond closely with the classical concepts, intensity and scale of segregation. The kinetics are remarkably similar to reversible crystal growth and breakage.[13,17] In fact, the resemblance of sandpile avalanches to first-order phase transitions has previously been noted.[15] Dimensionless variables minimize the number of parameters to α, β, and N, in addition to the initial conditions. The computed results are consistent with experimental observations and computer simulations showing exponential and power-law behavior at long times.

Notation

$c^{(n)}(t)$ = nth mass moment of the cluster size distribution
$C^{(0)}$ = dimensionless number concentration of clusters (Eq. 22)
$C^{(1)}$ = dimensionless mass concentration of clusters (Eq. 22)
C^{avg} = dimensionless average cluster size, also scale of segregation
$m(x, t)$ = single particle (monomer) number distribution
N = number of fragments in a cluster breakage event
S = dimensionless monomer concentration, also intensity of segregation (Eq. 22)
t = time
x = cluster mass
x_{m} = single particle (monomer) mass
α = dimensionless aggregation rate coefficient (Eq. 22)
β = dimensionless fragmentation rate coefficient (Eq. 22)
θ = dimensionless time (Eq. 22)

Subscripts

0 = initial condition
f = final condition ($t \to \infty$)

Literature Cited

1. Shinbrot T, Muzzio FJ. Nonequilibrium patterns in granular mixing and segregation. *Physics Today*. 2000;March:25.
2. Ottino JM, Khakhar DV. Fundamental research in heaping, mixing, and segregation of granular materials: Challenges and perspectives. *Powder Technol*. 2001;121:117–122.
3. Tegzes P, Vicsek T,Schiffer P. Development of correlations in the dynamics of wet granular avalanches *Phys. Rev. E*. 2003;67:051303.
4. Gray JMNT. Granular flow in partially filled slowly rotating drums. *J Fluid Mech*. 2001;441:1–29.
5. Ottino JM, Khakhar DV. Scaling of granular flow processes: From surface flows to design rules. *AIChE J*. 2002;48:2157–2166.
6. Kadanoff LP. Built upon sand: Theoretical ideas inspired by granular flows. *Rev. Mod. Phys*. 1999;71:435–444.
7. Jaeger HM, Nagel SR, Behringer RP. Granular solids, liquids, and gases. *Rev. Mod. Phys*. 1996;68:1259–1273.
8. McCarthy JJ, Khakhar DV, Ottino JM. Computational studies of granular mixing. *Powder Technol*. 2000;109:72–82.
9. Muzzio FJ. Powder technology in the pharmaceutical industry: The need to catch up fast. *Powder Technol*. 2002;124:1–7.
10. Knight JB, Fandrich CG, Lau CN, Jaeger HM, Nagel SR. Density relaxation in a vibrated granular material. *Phys. Rev. E*. 1995;51:3957–3963.
11. Sterling WJ, McCoy BJ. Distribution kinetics of thermolytic macromolecular reactions. *AIChE J*. 2001;47:2289–2303.
12. Madras G, McCoy BJ. Growth and ripening kinetics of crystalline polymorphs. *Crystal Growth Des*. 2003;3:981–990.
13. Madras G, McCoy BJ. Dynamics of crystal size distributions with size-dependent rates. *J. Crystal Growth*. 2002;243:204–213.
14. Madras G, McCoy BJ. Temperature effects for crystal growth: A distribution kinetics approach. *Acta Mater*. 2003;51:2031–2041.
15. Jaeger HM, Nagel SR. Physics of the granular state. *Science*. 1992;255:1523–1527.
16. Madras G, McCoy BJ. Population balance modeling of turbulent mixing for miscible fluids. in press, 2004.
17. McCoy BJ. A population balance framework for nucleation, growth, and aggregation. *Chem. Eng. Sci*. 2002;57:2279–2285.
18. Diemer RB, Olson JH. A moment methodology for coagulation and breakage problems: Part 3—Generalized daughter distribution functions. *Chem. Eng. Sci*. 2002;57:4187–4198.
19. Hill PJ, Ng MK. Statistics of multiple particle breakage. *AIChE J*. 1996;42:1600–1611.
20. Michaels AS, Puzinauskas V. Mechanical mixing processes: The dextrose–kaolinite–water system. *Chem. Eng. Prog*. 1958;50:604–614.
21. Brodkey RS. *The Phenomena of Fluid Motions*. Reading, MA: Addison–Wesley; 1967.
22. Weidenbaum SS. Mixing of solids. *Adv. Chem. Eng*. 1958;II:209–324.
23. Khakhar DV, McCarthy JJ, Shinbrot T, Ottino JM. Transverse flow and mixing of granular materials in a rotating cylinder. *Phys. Fluids*. 1997;9:31–43.
24. Khakhar DV, McCarthy JJ, Shinbrot T, Ottino JM. Radial segregation of granular mixtures in rotating cylinders. *Phys. Fluids*. 1997;9:3600–3614.